Formation of Interfaces in Incompatible Polymer Blends: A Dynamical Mean Field Study

Chuck Yeung*,† and An-Chang Shi‡

School of Science, The Behrend College, Pennsylvania State University at Erie, Erie, Pennsylvania 16536, and Xerox Research Centre of Canada, 2660 Speakman Drive, Mississagua, Ontario, Canada L5K 2L1

Received October 22, 1998; Revised Manuscript Received March 23, 1999

ABSTRACT: The interdiffusion dynamics of a polymer interface towards its equilibrium profile is studied using a dynamical mean field method, in which the nonequilibrium chemical potentials are evaluated numerically using the full polymer mean field free energy. Our results demonstrated that the interfacial width grows as $t^{1/4}$ at early times and saturates to the equilibrium thickness at long times, in agreement with previous, more approximate analysis based on Cahn−Hilliard-type theories. Furthermore, we show that the dynamical exponent can only be obtained unequivocally via a scaling analysis. The interdiffusion of a polymer interface in the single phase regime is also studied.

I. Introduction

Polymer blends are used in increasing areas of application because they are cost-effective and have the potential for design of materials with properties tailored to a specific use. Because most polymer blends are composed of immiscible polymers, many blend properties are determined by the characteristics of the interfaces between the different components. To obtain good mechanical properties, good cohesion between phases is required, and different materials have to interpenetrate into each other at the interfaces. This interpenetration depends on the degree of miscibility of components and is generally neither easy to determine experimentally nor easy to predict theoretically. This has led to an intensive effort to understand the static and dynamic properties of polymer interfaces.

The equilibrium properties of polymer interfaces are now relatively well-understood.[1] More recently interest has turned to the dynamics of polymer interfaces. In one set of experiments, a sharp interface between two polymer films was initially prepared,[2−5] and the broadening of the interface as the polymers interdiffuse was monitored via nuclear reaction analysis. These experiments found that the interdiffusion was subdiffusive with the interfacial width W growing as $W(t) \propto t^{\alpha}$, where the exponent α ranged from about 0.25 to 0.4. It was also found that the exponent α decreases as the temperature is lowered.[3]

All extant theoretical analysis of polymer interdiffusion starts from an approximate form for the coarse-grained free energy for a binary polymer blend,

$$F = \int \mathrm{d}\mathbf{r} \left[f_o(\phi) + \frac{\Lambda(\phi)}{2} |\nabla\phi|^2 \right] \tag{1}$$

where ϕ is the volume fraction of A polymers and Λ is taken to be either a constant or, more accurately for polymers, $\Lambda = \Lambda_o/[18\phi(1-\phi)]$. The local free energy density f_o is chosen to be either of the Flory−Huggins type[6,7] or a fourth-order expansion in terms of $\phi(\mathbf{r})$.[8,9] For the dynamics of the system, Puri and Binder[8] and Wang and Shi[9] assumed that the dynamics are approximated by the Cahn−Hilliard dynamics

$$\frac{\partial\phi(\mathbf{r}, t)}{\partial t} = \nabla\cdot\Gamma(\phi)\nabla\frac{\delta F}{\delta\phi(\mathbf{r}')} \tag{2}$$

where Γ is the mobility. On the other hand, Harden derived a more complicated nonlocal form for the dynamics

$$\frac{\partial\phi(\mathbf{r}, t)}{\partial t} = \int \mathrm{d}\mathbf{r}'\, \mathbf{\Gamma}(\mathbf{r}, \mathbf{r}')\cdot\nabla\frac{\delta F}{\delta\phi(\mathbf{r}')} \tag{3}$$

where $\mathbf{\Gamma}$ is a kernel derived from Gaussian dynamics.[7] Kawakatsu et al. has also performed a similar analysis using reptation dynamics.[12] Harden found that the interfacial width initially grows as $t^{1/2}$ followed by a $t^{1/4}$ growth regime. Puri and Binder also found that $W(t) \propto t^{1/4}$ before saturating at the equilibrium interfacial thickness.[8] On the other hand, a similar numerical analysis by Wang and Shi found that the exponent α depended on temperature with $\alpha < {}^1/_4$ for all cases and α decreasing to 0.10 for lower temperatures.[9]

The approximate form of the free energy used in these analysis almost guarantees that $W \propto t^{1/4}$ because the free energy expression (eq 1) is expanded to second order in $\nabla\phi$ so that the highest order gradient term in the dynamical equation (eq 2) is $\nabla^4\phi$. Simple dimensional analysis of eq 2 then gives $t^{-1} \propto W^{-4}$ or $W \propto t^{1/4}$. Such an expansion is appropriate close to the critical point but should not hold further away from the critical point. In general, the gradient expansion of the free energy functional must be expressed in the form of an infinite series, as shown recently by Tang and Freed.[10] Furthermore, it has been demonstrated that the square gradient approximation considerably overestimates the interfacial tension.[11] To understand the dynamics of the interfaces, it is desirable to develop a theory based on the *exact* free energy functional of the system. In this paper, the dynamics of polymer interfaces is studied using a dynamic mean field approach. Our theory adopts the numerical methods developed by Fraaije and coworkers[13−15] and by Hasegawa and Doi.[16,17] In this theory, the chemical potential $\delta F/\delta\phi$ is calculated from

† Pennsylvania State University at Erie.
‡ Xerox Research Centre of Canada.

10.1021/ma981648n CCC: $18.00
Published on Web 05/06/1999

the nonequilibrium free energy at each time step. The advantage of this method is that we can use a more microscopically valid free energy expression which can, for example, include features of the polymer architecture such as branches and blocks.[14,15]

Using this more exact method, we find that the interfacial width $W(t)$ grows as $t^{1/4}$ at early times, saturating to its equilibrium thickness at long times. These results agree with Puri and Binder[8] and the late time results of Harden.[7] We also find that a simple power law fit to $W(t)$ gives a exponent which decreases with separation from the critical point. Only when the data is collapsed via a scaling analysis is it possible to unequivocally identify the $t^{1/4}$ scaling. Finally, we study the widening of an interface following a quench from the two-phase to the one-phase regime. In this case, the interfacial thickness first grows as $W(t) \propto t^{1/4}$ followed by an asymptotic regime in which $W(t) \propto t^{1/2}$. This is again in agreement with the analysis by Puri and Binder and the experimental observation of subdiffusive behavior seen by May and Maher[18] for simple liquids near the critical point and those analyzed by Ma et al.[19]

II. Dynamical Mean Field Theory

The free energy functional of a polymer blend is obtained from the Edwards model of the polymers. Following Hong and Noolandi,[21] we write the partition function for incompressible binary polymer blend in terms of the volume fractions ϕ_a and ϕ_b and their conjugate fields ω_a and ω_b,

$$Z = \int \prod_{p=a,b} D\{\phi_p(\mathbf{r})\}\, D\{\omega_p\} e^{-F\{\omega,\phi\}} \tag{4}$$

where the energy is written in units of $k_B T$. The free energy $F\{\phi, \omega\}$ can be divided into two parts as $F\{\phi, \omega\} = F_o\{\phi, \omega\} + F_1\{\phi, \omega\}$. The independent chain free energy F_o is given by

$$e^{-F_0\{\omega\}} = \prod_{p=a,b} \times \left(\frac{Z_{\mathrm{kin},p}^{N_p}}{N_p!} \int D\{\mathbf{R}_p\} P_o\{\mathbf{R}_p\} e^{-\sum_{p=a,b} \int \mathrm{d}\mathbf{r}\, \omega_p(\mathbf{r}) \hat{\phi}_p(\mathbf{r})} \right) \tag{5}$$

where $Z_{\mathrm{kin},p}$ is the kinetic portion of the single chain partition function, N_p is the number of p type polymers, and $\hat{\phi}$ is a functional of the chain conformation

$$\hat{\phi}_p(\mathbf{r}) = \sum_{j=1}^{N_p} \int_0^{Z_p} \mathrm{d}t\, \delta[\mathbf{r} - \mathbf{R}_{pj}(t)] \tag{6}$$

P_o is the chain conformation probability,

$$P_o\{\mathbf{R}_{pj}\} = \exp\left(-\frac{3}{2} \int_0^{Z_p} \mathrm{d}t \left| \frac{\partial \mathbf{R}_{pj}}{\partial t} \right|^2 \right) \tag{7}$$

where we have written all lengths in terms of the monomer size b. The interaction portion of the free energy is given by

$$F_1\{\omega, \phi\} = \int \mathrm{d}\mathbf{r} \left\{ -\sum_{p=a,b} \omega_p(\mathbf{r}) \phi_p(\mathbf{r}) + f_{\mathrm{int}}[\phi(\mathbf{r})] \right\} \tag{8}$$

Note that ω_p is essentially the potential for polymer p. The interaction energy is given by

$$f_{\mathrm{int}}(\phi) = \chi \phi_a(\mathbf{r}) \phi_b(\mathbf{r}) \tag{9}$$

where χ is the dimensionless Flory−Huggins parameters and v is the volume per monomer.

The method introduced by Fraaije is essentially to use the Cahn−Hilliard dynamics with the full mean field free energy.[13] Taking the interface to be in the $x-y$ plane and neglecting any fluctuations in the plane, the dynamics for the polymer concentrations $\phi(z, t)$ is

$$\frac{\partial \phi_a}{\partial t} = -\frac{\partial \phi_b}{\partial t} = \frac{\partial}{\partial z} \Gamma(\phi) \frac{\partial}{\partial z} \mu_{ab} \tag{10}$$

where the mobility $\Gamma(\phi)$ is given by

$$\Gamma(\phi) = \phi_a \phi_b$$

The chemical potential difference $\mu_{ab}(z)$ is

$$\mu_{ab}(z) = \frac{\partial F}{\partial \phi_a(z)} - \frac{\partial F}{\partial \phi_b(z)} = \omega_a(z) - \omega_b(z) + \chi\,[\phi_b(z) - \phi_a(z)] \tag{11}$$

The potentials $\omega_p(z)$ are determined by requiring $\partial F / \delta \omega_p(z) = 0$. This gives the usual mean field expression relating the volume fraction ϕ_p to the independent chain Green's function G_p,

$$\phi_p(z) = \frac{\bar{\phi}_p}{Z_p} \frac{\int_0^Z \mathrm{d}s\, G_p(z, s) G_p^\dagger(z, Z_p - s)}{Q_p} \tag{12}$$

where $\bar{\phi}_p$ is the average of ϕ_p over the volume. The independent chain partition function Q_p is a functional of ω

$$Q_p(\{\omega\}) = \int \mathrm{d}z\, G_p(z, Z_p) \tag{13}$$

The end-integrated independent chain Green's function $G_p(z, s)$ is also a functional of ω and obeys

$$\frac{\partial G_p(z, s)}{\partial s} = \frac{1}{6} \frac{\partial^2}{\partial z^2} G_p(z, s) + \omega_p(z) G_p(z, s) \tag{14}$$

with the initial conditions $G_p(z, 0) = 1$ and $G_p^\dagger(z, Z - s) = G_p(z, s)$.

III. Numerical Method

To simplify our analysis, we consider a symmetric binary blend so that $Z_a = Z_b = Z$. We discretize a system of size L into a mesh of size $\Delta x = 0.5$. In our simulations, we varied L from 100 to 200 depending on the polymerization Z. We confirmed that our results were mesh-size- and system-size-independent by varying Δx and L.

At the start of each run, we prepared a sharp interface between A- and B-rich phases with the two bulk phases given by the values of ϕ on the coexistence curve. This gives the initial value of $\phi(z)$ for use in the dynamical update equation (eq 10). The update requires the calculation of the chemical potential difference μ_{ab} and hence ω_a and ω_b at each time step. The numerical difficulty arises because eq 12 cannot easily be inverted to obtain $\omega_p(z)$ from the given $\phi_p(z)$. Therefore, we must determined ω_p numerically. We used a combination gradient-descent/secant method to determine ω. This required the calculation of the derivative matrix $d\phi_p$-

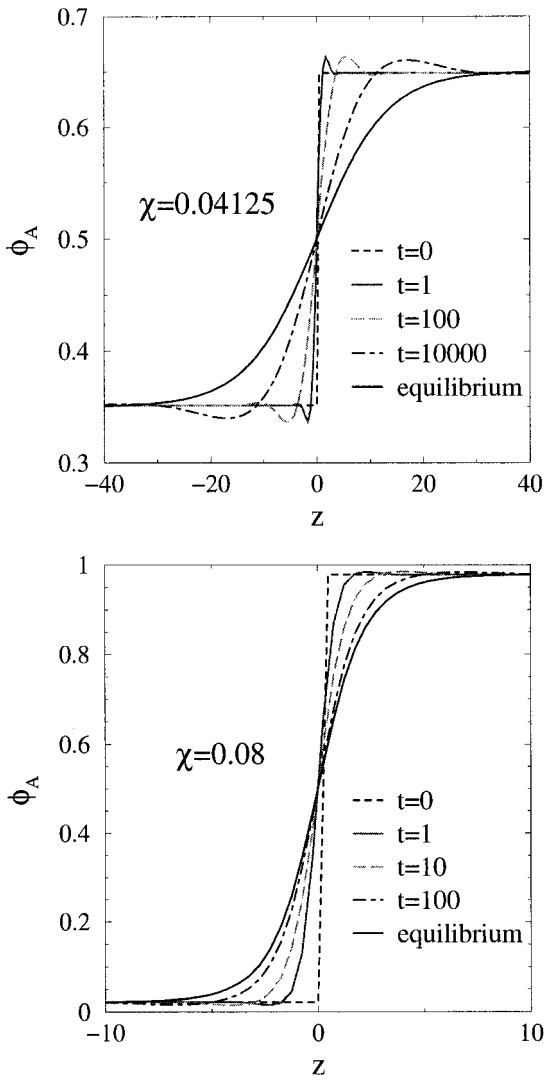

Figure 1. *A* volume fraction ϕ_A at different times for $Z = 50$ for weak segregation (top: $\chi = 0.04125$) and strong segregation (bottom: $\chi = 0.08$). The *B* concentration is not shown because it is a mirror image of ϕ_A. Here z is measured in terms of monomer lengths.

$(z)/d\omega_p(z')$ numerically. The calculation of this matrix is extremely computationally expensive but could be done infrequently. We required that our solution for ω_p-(z) gave a $\phi_p(z)$ that did not vary by more than 10^{-6} from its actual value at any point z.

We then integrated the dynamical equation using an Adams−Bashford method. The time step was varied with a smaller time step chosen at early times when the interface width is thinner. We then repeated the procedure for different values of χ and chain length Z to determine the behavior in both strong and weak segregation regimes.

IV. Results and Discussions

A. Lengthscale. Figure 1 shows examples of the time evolution of the density profiles, in which the values of $\phi_A(z)$, the volume fraction of *A* polymer, at different times for both weak segregation $\chi = 0.04125$ (top) and strong segregation $\chi = 0.80$ (bottom) are presented. The interface is at $z = 0$ and the critical χ is $\chi_c = {}^2/_Z = 0.04$. Only $\phi_A(z)$ is shown, because $\phi_B(z)$ is a mirror image of ϕ_A. At $t = 0$, the *A*- and *B*-rich bulk phases are brought into contact to produce an initially sharp interface. The

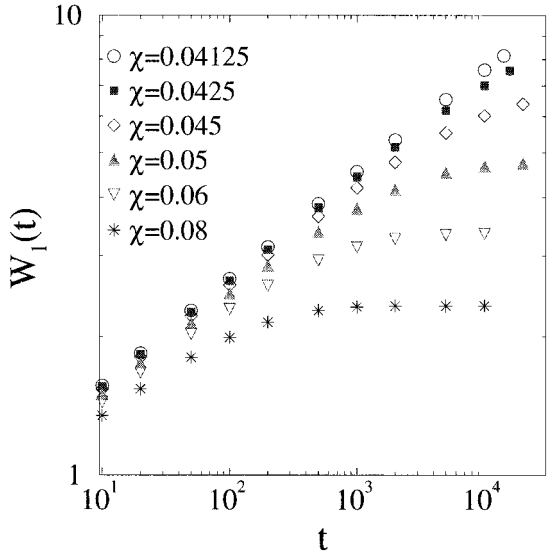

Figure 2. Interfacial width defined as the inverse of the maximum slope of $\phi_A(z)$ for fixed $Z = 50$ and different values of χ. A power law fit to the early times leads to an exponent that depends on χ.

interface broadens as the *A* polymers diffuse from the *A*-rich to the *A*-poor phase. The broadening is fast initially but slows as the interface approaches its equilibrium profile.

This behavior is similar to that observed in earlier studies using the Cahn−Hilliard equation and a gradient-expansion free energy.[8,9] However, one feature that has not been previously reported is that there is a small region on the *A*-rich side near the interface in which $\phi_A(z)$ is enhanced above its equilibrium bulk value. The bump still exists for larger χ but the enhancement is necessarily smaller and therefore more difficult to observe. We will return to a discussion of this enhanced concentration region later.

Figure 2 shows the interfacial width W as a function of time for $Z = 50$. Here, we chose a sequence of χ ranging from weak to strong segregation. As a quantitative measure of the interfacial width, we followed Steiner et al.[3] and chose the inverse of the maximum slope of ϕ_A at the interface,

$$W_1(t) = \left(\frac{1}{\Delta\phi_A}\left.\frac{\partial\phi_A}{\partial z}\right|_{z=0}\right)^{-1} \tag{15}$$

where $\Delta\phi_A$ is the difference between the bulk values of ϕ_A in the two equilibrium phases. This definition is sensitive to the local structure of the interface. We also determined a second measure of the interfacial width which is related to the surface tension. This measure, $W_2(t)$, takes into account the entire structure of the interface

$$W_2(t) = \left(\frac{1}{\Delta\phi_A}\int_{-\infty}^{\infty} \mathrm{d}z \left|\frac{\partial\phi_A}{\partial z}\right|^2\right)^{-1} \tag{16}$$

We found that these two measures essentially scale with each other, so we will only report the results for W_1.

As shown in Figure 2, there is no clear regime in which $W(t)$ grows as a power law except for χ near the critical point. At early times, the results depend on the initial condition. At late times, the interfacial width saturates to its equilibrium value. Therefore, to fit a

Table 1. Dynamical Exponents α Obtained from a Power Law Fit to $W(t) \propto t^{\alpha}$ for Fixed $Z = 50$[a]

χ	$Z(\chi - \chi_c)$	α
0.041 25	0.0625	0.2322 ± 0.0005
0.042 5	0.125	0.230 ± 0.001
0.045	0.25	0.225 ± 0.001
0.05	0.5	0.216 ± 0.002
0.06	1.0	0.195 ± 0.005
0.08	2.0	0.157 ± 0.008

[a] Five data points from $t = 10$ to $t = 200$ of each set were used in the fit. The value of α obtained from this fit decreases with increasing χ.

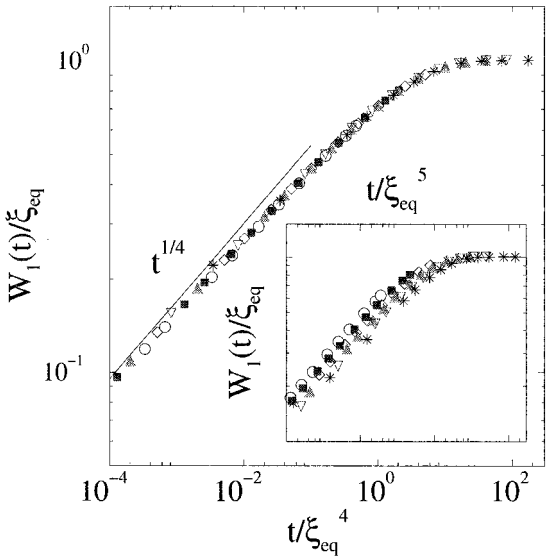

Figure 3. Data from Figure 2 plotted in a scaled form. Here $W_1(t)$ is scaled by the equilibrium interfacial width ξ_{eq} and the time by ξ_{eq}^4. The data collapse onto a single master curve. The inset is the same data with time scaled by ξ_{eq}^5. In this case, the data no longer collapse well.

power law, one must arbitrarily choose a range in which the data approximate a straight line on a log−log plot. The exponent α is then obtained from a fit to the log−log plot. Table 1, shows the value of α obtained from a power law fit to five data points between $t = 10$ and $t = 200$. As shown in Table 1, the exponent α obtained from this procedure depends on χ with α decreasing from 0.23 to 0.16 with increasing χ. This behavior is very similar to the results observed by Wang and Shi[9] as they found that the exponent α is always less than $^1/_4$ and decreases with increasing χ. Experimentally, Steiner et al.[3] also found the exponent decreases with increasing χ, although in that case they found exponents ranging from 0.25 to about 0.4.

Therefore, a straightforward power law fit may not illuminate the scaling behavior. To show the scaling behavior more clearly, we use a technique from critical phenomena[20] and assume that $W(t)$ is governed by a master function

$$W_1(t) = \xi_{eq} f(t/\xi_{eq}^{1/\alpha}) \tag{17}$$

where f is a dimensionless function with $f(\infty) = 1$ and ξ_{eq} is the equilibrium interfacial thickness. If this form holds, then a plot of $W_1(t)/\xi_{eq}$ versus $t/\xi_{eq}^{1/\alpha}$ will collapse onto a single curve.

Figure 3 shows the scaling plot using the same data as in Figure 2 and assuming $\alpha = ^1/_4$. We see that even the large χ data collapse well onto a single master curve,

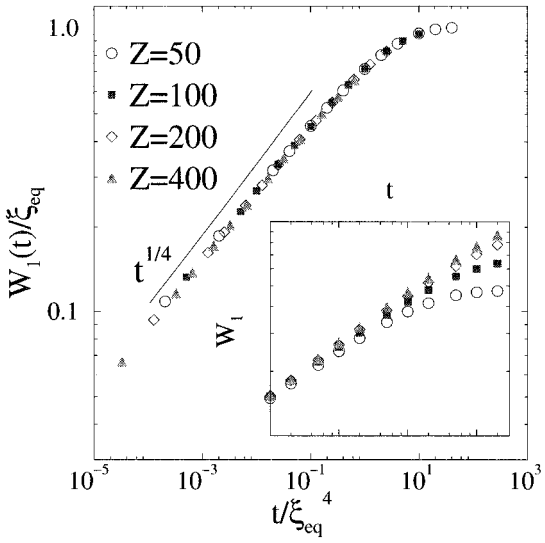

Figure 4. $W_1(t)$ for different Z's at fixed $Z\chi$ plotted in a scaled form W_1/ξ_{eq} vs. t/ξ_{eq}^4. The inset is the same data plotted in the original unscaled form, $W_1(t)$ vs t. Again, we see that the scaled data collapse onto a single master curve.

indicating that the dynamical exponent is independent of χ and is close to $^1/_4$ over the entire range of χ. Therefore, the χ dependence of α observed previously,[3,9] is most likely an artifact due to the fit of α to the limited power law region at larger χ. The inset of Figure 3 shows an attempt to scale the same data assuming $\alpha = ^1/_5$. We see that the data no longer collapses onto a single curve. Therefore, we can rule out $\alpha = ^1/_5$ for the dynamical exponent.

In our first set of calculations, we fixed Z and varied χ. To study the effect of chain length Z, we also considered a sequence of Z with the product $Z\chi = 2.5$ fixed so that the bulk equilibrium values are fixed. We perform the analysis for $Z = 50$ ($\chi = 0.05$), $Z = 100$ ($\chi = 0.025$), $Z = 200$ ($\chi = 0.0125$), and $Z = 400$ ($\chi = 0.00625$). Figure 4 shows the scaling plot of the interfacial width $W_1(t)/\xi_{eq}$ versus t/ξ_{eq}^4 for the four sets of data for fixed $Z\chi$. The inset shows the initial unscaled data. We see again that the scaled data collapse well onto a single curve, indicating that the dynamical exponent is close to $^1/_4$ and is independent of Z.

To study the effect of the mobility Γ, we also performed the same analysis for constant $\Gamma = 1$ instead of $\Gamma = \phi_A\phi_B$. This is the usual assumption when writing the Cahn−Hilliard dynamics for simple liquids. We find that the scaling behavior with constant Γ is the same as discussed above except that the equilibrium profile is reached approximately 4 times earlier because $\phi_A\phi_B = ^1/_4$ at the interface ($z = 0$).

Finally, we consider how a sharp interface disappears when the system is brought into the single-phase regime. For our initial state, we start with a sharp interface with fixed $\chi Z = 2.5$ and Z varying from 25 to 200. We then instantaneously change χ to 0, corresponding to high temperature, and allow the polymers to interdiffuse. In each case, we observe that the interfacial width grows initially as $W \propto t^{1/4}$ followed by a late time regime in which the interface spreads diffusively as $W(t) \propto t^{1/2}$.

This is shown in the inset of Figure 5 and is consistent with the analysis of Puri and Binder[8] as well as Ma et al.[19] for simple liquids. In this case, the scaling length must be the equilibrium correlation length, which for χ

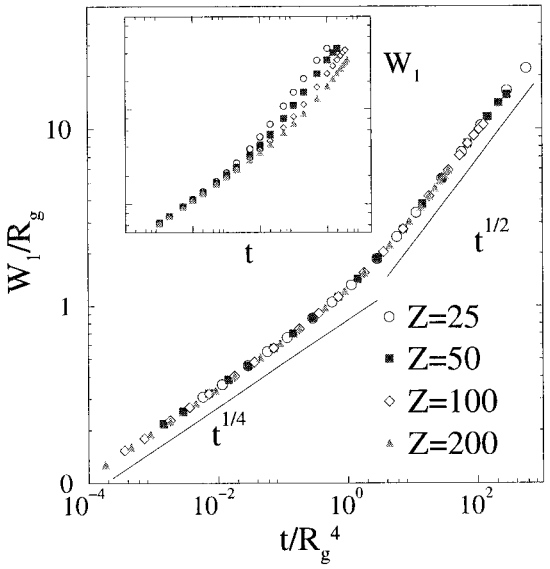

Figure 5. Plot of the interfacial width showing the broadening of the interface after an initially sharp interface is taken into the single-phase regime ($\chi = 0$). Here there is a $t^{1/4}$ growth regime followed by $t^{1/2}$ growth. As seen from the figure, the crossover occurs at the equilibrium length $\xi_{eq} \propto R_g$.

$= 0$ is given by $\xi_{eq} \propto R_g = (Z/6)^{1/2}$.[22] Therefore the scaling function must be of the form

$$W(t) = R_g\, g(t/R_g^4) \tag{18}$$

where $g(x)$ is a dimensionless scaling function. Figure 5 shows the single-phase data plotted in this scaling form. Again, we see excellent collapse of the data, indicating that the assumed scaling form holds. We also see that the scaling function behaves as $g(x) \propto x^{1/4}$ for $x \ll 1$ and $g(x) \propto x^{1/2}$ for $x \gg 1$, indicating that $W(t) \propto t^{1/4}$ for $W \ll \xi_{eq}$ and $W(t) \propto t^{1/2}$ for $W \gg \xi_{eq}$.

B. Enhanced Concentration Region. We now return to the region near the interface observed in Figure 1 where the ϕ_A is enhanced above the bulk coexistence value on the *A*-rich side and depleted below the other bulk coexistence value on the *B*-rich side. We will concentrate on the weak segregation case with $\chi = 0.04125$ and $Z = 50$. In the weak segregation regime, the simple coarse-grained free energy given in eq 1 should be a reasonable approximation to the full free energy. This is further indicated in the figure because at $t = 10\,000$, the bump is at $z \propto 20$, which is about 7 times the radius of gyration, indicating that chain connectivity should not be important.

The origin of the ϕ-enhanced/depleted bumps can be understood based on symmetry. Taking the interface to be at $z = 0$, the chemical potential $\mu = \delta F/\delta\phi$ is an odd function of z with $\mu = 0$ at $z = \pm\infty$ and at $z = 0$. This implies that there is a maximum in the chemical potential in the *A*-rich side of the interface and a minimum in the *A*-poor side. The order-parameter current is related to μ via $j_z = -M(\phi)\mathrm{d}\mu/\mathrm{d}\phi$. Near the interface, ϕ will be transported from the ϕ-rich side to the ϕ-poor side. However, j_z must change signs where μ is extremized. Therefore, at a sufficiently far distance from the interface, j_z must transport ϕ away from the interface on the ϕ-rich side and toward the interface on the ϕ-poor side. This leads to the enhancement of ϕ above the equilibrium value on the *A*-rich side and a depletion on the *A*-poor side observed in the simulations.

To test this idea, we return to the simple coarse-grained free energy for a symmetric polymer blend given in eq 1 with $f_o(\phi) = \chi\phi(1-\phi) + \phi\log(\phi)/Z + (1-\phi)\log(1-\phi)/Z$. We start with a sharp interface using the same values of χ and Z as those for the full polymer free energy and updated the concentration profile using eq 2. Again, we find an enhanced and depleted region which moves away from the interface with time, indicating that the bump is also present in simple molecules.

V. Conclusion

We have studied the broadening of a polymer interface from an initially sharp interface using a numerical dynamical mean field method recently introduced by Fraaije et al. and Hasegawa and Doi. In this method the nonequilibrium chemical potentials are evaluated numerically using the full polymer mean field theory. Therefore, we do not have to rely on a gradient expansion of the free energy which must give the $W(t) \sim t^{1/4}$ growth. Our results are in agreement with the gradient-expansion analysis of Puri and Binder, which predicts that the interfacial width $W(t)$ grows as $t^{1/4}$ at early times. However, away from the critical point, the power law regime is limited, so that a simple power law fit to the data will give a χ-dependent exponent. We show that the data must be plotted in a scaling form to clearly identify the scaling exponent. We show that $t^{1/4}$ scaling is observed even away from the critical point. We also study the broadening of an initially sharp interface after a quench into the single-phase regime. There is a initial $t^{1/4}$ subdiffusive regime followed by a $t^{1/2}$ late time diffusive regime. The cross-over occurs at the equilibrium correlation length.

Acknowledgment. C.Y. gratefully acknowledges support for this work from the Research Corporation under Cottrell College Science Grant CC3993. C.Y. would also like to thank Ken Bauer for providing some of the computational resources.

References and Notes

(1) For example, see: Sanchez, I. C. *Physics of Polymer Surfaces and Interfaces*; Butterworth-Heinemann: Boston MA, 1992.
(2) Chaturvedi, U.; Steiner, U.; Zak, O.; Krausch, G.; Klein, J. *Phys. Rev. Lett.* **1989**, *63*, 616.
(3) Steiner, U.; Krausch, G.; Schatz, G.; Klein, J. *Phys. Rev. Lett.* **1990**, *64*, 1119.
(4) Klein, J. *Science* **1990**, *250*, 640.
(5) Losch, A.; Woerman, D.; Klein, J. *Macromolecules* **1994**, *27*, 5714.
(6) de Gennes, P. G. *C. R. Acad. Sci.* **1989**, *B308*, 13.
(7) Harden, J. L. *J. Phys. (Paris)* **1990**, *51*, 1777.
(8) Puri, S.; Binder, K. *Phys. Rev. B* **1991**, *44*, 9735.
(9) Wang, S. Q.; Shi, Q. *Macromolecules* **1993**, *26*, 1091.
(10) Tang, H.; Freed, K. F. *J. Chem. Phys.* **1991**, *94*, 1572.
(11) Ermoshkin, A. V.; Semenov, A. N. *Macromolecules* **1996**, *29*, 6294.
(12) Kawakatsu, T. *Phys. Rev. E* **1997**, *56*, 3240.
(13) Fraaije, J. G. E. M. *J. Chem. Phys.* **1993**, *99*, 9202.
(14) Maurits, N. M.; Fraaije, J. G. E. M. *J. Chem. Phys.* **1997**, *107*, 15879.
(15) Maurits, N. M.; Fraaije, J. G. E. M. *J. Chem. Phys.* **1997**, *106*, 6370. Maurits, N. M.; van Vlimmeren, B. A. C.; Fraaije, J. G. E. M. *Phys. Rev. E* **1997**, *56*, 816. Zvelindovshy, A. V.; Sevink, G. J. A.; van Vlimmeren, B. A. C.; Maurits, N. M.; Fraaije, J. G. E. M. *Phys. Rev. E* **1998**, *57*, 4879.
(16) Hasegawa, R.; Doi, M. *Macromolecules* **1991**, *30*, 3086.
(17) Hasegawa, R.; Doi, M. *Macromolecules* **1997**, *30*, 5490.

(18) May, S. E.; Maher, J. V. *Phys. Rev. Lett.* **1991**, *67*, 2013.
(19) Ma, W. J.; Keblinski, P.; Maritan, A.; Koplik, J.; Banavar, J. R. *Phys. Rev. Lett.* **1993**, *71*, 3465.
(20) For example, see: Ma, S. K. *Theory of Critical Phenomena*; Benjamin Press, 1976.
(21) Hong, K. M.; Noolandi, J. *Macromolecules* **1981**, *14*, 727.
(22) Doi, M.; Edwards, S. F. *The Theory of Polymer Dynamics*; Oxford University Press: London, 1986.

MA981648N